phase-angle deviations given above are only indications of the accuracy of the refinement procedure. The overall errors in the determined phase values are about 30° and come mainly from the intensity fluctuation caused by the beam instability and the overlapping of adjacent weak multiple diffractions. It is worth mentioning that, because of the low X-ray power used, the sample crystal did not deteriorate after six months of X-ray exposure.

Concluding remarks

To sum up, we have demonstrated the possibility of using conventional in-house X-ray sources to carry out multiple diffractions for the phase determination of macromolecular crystals. In addition, we have shown that the use of direct-beam optics without a monochromator, the repetition of the ψ scan and the adoption of a vertical axis for the detector have greatly improved the visibility of the multibeam interaction effect on the diffraction intensity. With this improvement, multiple-diffraction experiments for solving the X-ray phase problem in macromolecular crystals are not limited to the use of synchrotron radiation. Moreover, many more useful phases can be obtained in a relatively longer period of time before the crystal deteriorates.

The authors are indebted to the National Science Council for financial support. MTH and CMW are grateful to the same organization for a postdoctoral fellowship and a graduate scholarship, respectively. The supply of lysozyme crystals by Mr Chia-Kuei Wu of the Institute of Molecular Biology, Academia Sinica and useful discussion with Professor B. C. Wang of the University of Pittsburgh are also gratefully acknowledged.

References

Chang, S. L., King, K. E., Huang, M. T. & Gao, Y. (1991). *Phys. Rev. Lett.* **67**, 3113–3116.
Chang, S. L., Tsai, Y. S. & Huang, M. T. (1993). *Phys. Lett.* A**177**, 61–66.
Diamond, R., Phillips, D. C., Blake, C. C. F. & North, A. C. T. (1974). *J. Mol. Biol.* **82**, 371–391.
Hümmer, K., Bondza, H. & Weckert, E. (1991). *Z. Kristallogr.* **195**, 169–188.
Hümmer, K., Schwegle, W. & Weckert, E. (1991). *Acta Cryst.* A**47**, 60–62.
Hümmer, K., Schwegle, W. & Weckert, E. (1992). *Acta Phys. Pol.* A**82**, 83–102.
Moon, R. M. & Shull, C. G. (1964). *Acta Cryst.* **17**, 805–812.

Acta Cryst. (1994). A**50**, 344–351

Disorder and the Molecular Packing of C_{60} Buckminsterfullerene: a Direct Electron-Crystallographic Analysis

By Douglas L. Dorset and Mary P. McCourt

Electron Diffraction Department, Medical Foundation of Buffalo, Inc., 73 *High Street, Buffalo, NY* 14203, *USA*

(*Received* 9 *August* 1993; *accepted* 10 *November* 1993)

Abstract

The crystal structure of C_{60} buckminsterfullerene was determined at room temperature by a direct phasing analysis of single-crystal electron-diffraction intensity data. The initial electrostatic potential map is well fit by a regular icosahedron of C atoms but with an average rotational disorder corresponding to $Fm\bar{3}m$ symmetry. The static appearance of this directly determined map, however, does not refute the notion of uncorrelated molecular positions in the crystal lattice, indicated earlier by nuclear-magnetic-resonance spectroscopy and neutron scattering. Although the direct determination of crystallographic phases is correct, the occurrence of strong axial $h00$ reflections in the electron diffraction patterns appears to be a result of secondary scattering. Correction for this perturbation produces a good fit of the intensities to an isotropic spherical shell of C atoms. In fact, the static appearance of the initial potential map is artificial, owing to the use of only a limited set of phased structure factors in the Fourier transform carried out after the *ab initio* structure analysis.

Introduction

Since the discovery of C_{60} buckminsterfullerene (Kroto, Heath, O'Brien, Curl & Smalley, 1985), considerable effort has been made to characterize the molecular packing in the solid state of this unusual form of carbon, which has been found to exist naturally (Daly, Busek, Williams & Lewis, 1993). X-ray and neutron diffraction analyses have shown that the room-temperature form crystallizes in space group *Fm*3*m*, with a disordered *Fm*3 packing (Fleming *et al.*, 1991). Below 249 K, a phase transition begins (Heiney *et al.*, 1991), transforming the face-centered-cubic packing to simple cubic packing, in space group *Pa*3, as seen in its crystal structure (Liu, Lu, Kapes & Ibers, 1991; David *et al.*, 1991). Electron diffraction and high-resolution electron microscopy have been used to characterize the various kinds of disorder found in these crystal structures (Krätschmer, Lamb, Fostiropoulos & Huffmann, 1990; Van Tendeloo, Op de Beeck, Amelinckx, Bohr & Krätschmer, 1991; Disko *et al.*, 1991; Ishiguro & Hirotsu, 1992; Saito, Suzuki, Shinohara, Hayashi & Tomita, 1992; Li, Zhao, Li, Zhu, Gan & Yin, 1992; Yao, Klein, Behal, Disko, Sherwood & Cox, 1992; Muto, Van Tendeloo & Amelinckx, 1993). While it is clear that the perfection of the crystal packing depends largely on the crystallization procedure used to prepare the specimen, a common feature of most crystals is the presence of stacking faults along the [111] direction in the room-temperature form.

These stacking faults, as well as a static disorder of the molecular packing [originally proposed to be a twinning mechanism (Fleming *et al.*, 1991)], have created some difficulties for quantitative crystallographic analyses, particularly of the room-temperature phase. For example, accurate bond lengths for the C_{60} molecule had only been obtained crystallographically from molecular derivatives (Hawkins, Mayer, Lewis, Loren & Hollander, 1991; Fagan, Calabrese & Malone, 1991; Birkett, Hitchcock, Kroto, Taylor & Walton, 1992; Tebbe *et al.*, 1992) until the low-temperature structure was solved (Liu, Lu, Kapes & Ibers, 1991) but similar bond lengths had been obtained previously by nuclear magnetic resonance (NMR) spectral simulation (Johnson, Bethune & Yannoni, 1992). In addition to the lattice perturbations already mentioned, there is yet another possible disorder that could seriously affect the outcome of a crystallographic analysis of the room-temperature form. That is to say, dynamic rotational freedom for the molecule noted in solid-state ^{13}C NMR experiments (Yannoni, Johnson, Meijer, Bethune & Salem, 1991; Tycko, Haddon, Dabbagh, Glarum, Douglass & Mujsce, 1991) would also contribute to the difficulty in determining the room-temperature structure by crystallographic analyses (Johnson, Bethune & Yannoni, 1992). At ambient temperature, the spectrum is a single narrow band, virtually identical to that obtained from a solution; *only* well below the subambient phase transition is this spectrum broadened. Quasielastic neutron scattering data (Neumann *et al.*, 1991; Copley *et al.*, 1992) also contain a strong diffuse signal at room temperature. The presence of a Lorentzian component was interpreted to be caused by the dynamic part of the total thermal diffuse scattering. As discussed by Fleming *et al.* (1991), this solid-state molecular motion could either be isotropic or a 'ratcheting' between symmetry-equivalent positions, perhaps, in the latter case, explaining the large Debye–Waller parameters found in the room-temperature X-ray analysis. However, more recent NMR measurements (Tycko, Dabbagh, Fleming, Haddon, Makija & Zahurak, 1991) suggest that such a hopping motion between relatively deep potential wells is possible only at low temperature. Nevertheless, simulations of high-resolution electron micrographs at molecular resolution (Wang & Busek, 1991) do not require incorporation of isotropic molecular motion into the model. A synchrotron X-ray study of single crystals (Chow *et al.*, 1992) also does not support the model of totally uncorrelated packing at room temperature.

Because significant questions remain about the nature of the ambient molecular packing of C_{60} buckminsterfullerene, it is clear that additional information might be obtained from a quantitative *ab initio* crystal structure analysis based on electron diffraction intensity data from thin microcrystals. It has been shown recently (Dorset, 1991, 1993), for a variety of materials, that 'direct methods' for crystallographic phase determination (Hauptman, 1972; Schenk, 1991) often permit successful structure analyses to be carried out with electron diffraction intensities, even though these data may be somewhat perturbed by multiple scattering. This prognosis is particularly relevant for molecular crystals, where the light-atom contents favor collection of a 'quasi-kinematical' data set (Dorset, Jap, Ho & Glaeser, 1979; Jap & Glaeser, 1980; Tivol, Dorset, McCourt & Turner, 1993), *i.e.* the measurement of intensities adequately near the single scattering approximation to permit the *ab initio* determination.

Materials and methods

Diffraction studies

Three-dimensional single-crystal electron diffraction intensity data were obtained from thin crystalline layers of C_{60} grown by evaporation of a dilute solution of buckminsterfullerene in benzene onto carbon-film-covered electron-microscope grids. The sample used for this study was purchased from the Aldrich Chemical Co. (Milwaukee, WI, USA) and was used without further purification. The crystals were mainly observed as the [111] orientation described previously by various authors. As discussed recently (Agafonov *et al.*, 1992), the crystals are probably solvent free. Selected-area electron diffraction patterns obtained at 100 kV with a JEOL JEM-100 CXII electron microscope were recorded on Kodak DEF-5 film, with precautions taken to minimize exposure of the sample to radiation. They are identical in appearance to those obtained from crystals grown by sublimation (Yao *et al.*, 1992). With the ±180° rotation holder for a side-entry ±60° tilt goniometer stage, it was possible to record patterns from the following projections: [111] (0° tilt), [211] (20° tilt), [123] (22° tilt), [110] (35° tilt), [310] (43° tilt) and [100] (55° tilt), resulting in a totally accessible unique data set of 42 reflections, extending to $\sin\theta/\lambda = 0.40$ Å^{-1}. Diffraction spacings were calibrated with an internal gold powder diffraction standard from an evaporated layer of the metal deposited on one edge of the sample grid. Diffraction intensities were measured by integration of peaks after films were scanned with a Joyce–Loebl Mk III C flat-bed microdensitometer; relative structure-factor magnitudes were taken as the square root of this measured intensity (see Dorset, 1976). Before intensity values were accepted from any crystal projection, patterns from several crystals were compared to ensure that the zonal data were internally consistent. These were then combined into a three-dimensional set as described by Hu & Dorset (1989).

Direct phase determination

Direct phase determination is based on the prediction of linear combinations of crystallographic phases: $\varphi = \phi_{\mathbf{h}(1)} + \phi_{\mathbf{h}(2)} + \phi_{\mathbf{h}(3)} + \dots$, with the constraint on Miller indices: $\sum_i \mathbf{h}(i) \equiv \sum_i h_i k_i l_i = 0,0,0$ (see Hauptman, 1972). These linear sums can be ranked in order of their descending probability of being correctly predicted. After the observed intensities are converted to normalized structure factors, $|E_h|^2 = I_{\rm obs}/\varepsilon \sum f_i^2$. [Here, ε accounts for translational symmetry and the f_i are the electron scattering factors for atomic components i (Doyle & Turner, 1968).] For example, so-called $\sum_2$ three-phase invariants ('triples') are ranked according to $A = (2/N^{1/2}) \times |E_{h(1)} E_{h(2)} E_{h(3)}|$ and a similar quantity can be calculated for the four-phase invariants ('quartets'). One is permitted to specify the phase of a limited number of reflections with appropriate Miller-index parity to define the unit-cell origin (see Rogers, 1980). One can also assign n additional algebraic values to other reflections with no index-parity restrictions so that 2^n maps must be generated for a centrosymmetric structure. These starting phase values are then used with the phase-invariant sums to find values for new phases, hopefully enough to permit calculation of an interpretable potential map. The application of direct methods to electron diffraction data has been discussed in two recent reviews (Dorset, 1991, 1993).

Initial structure analysis

Examination of diffraction data from various projections reveals that the unit cell is cubic, with a measured lattice constant $a = 14.26\,(23)$ Å, in good agreement with the 14.20 Å value measured earlier (Fleming *et al.*, 1991). As discussed extensively in earlier work (Ishiguro & Hirotsu, 1992; Saito *et al.*, 1992; Li *et al.*, 1992; Yao *et al.*, 1992), the weak reflections in diffraction patterns from the untilted [111] projection are caused by an extensive layer-stacking disorder. We have demonstrated this experimentally by a continuous tilt series with the electron-microscope goniometer stage, *e.g.* around the $\mathbf{d}^*_{\bar{1}10}$ reciprocal axis, wherein no diffraction intensities are ever found to vanish along a reciprocal-lattice row parallel to [111]. For our initial quantitative structure analyses, we have chosen 36 unique diffraction data from the [110] projection (Fig. 1), which correspond to the *cmm* plane-group symmetry required for either *Fm*3 or *Fm*3*m* (Henry & Lonsdale, 1969). These intensity data also have the advantage of originating from a projection that is identical for both space groups if one accepts the static disorder or 'twinning' mechanism of Fleming *et al.* (1991). Because the number of symmetry operations is halved, we have decided to carry out initial analyses in the lower-symmetry space group.

It was our intent to visualize the molecular structure without presuming any features from any previous determination. Accordingly, crystallographic

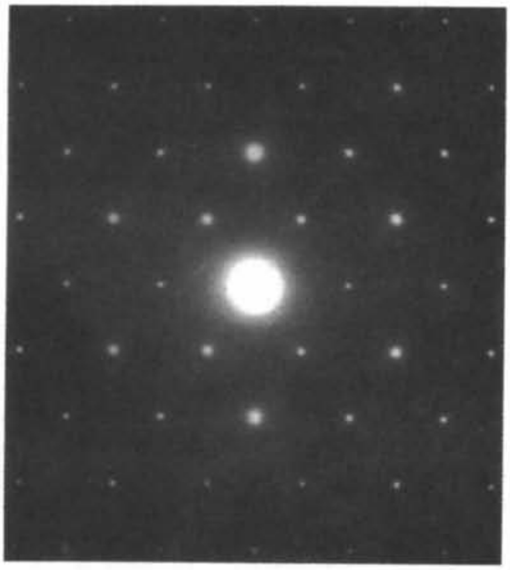

Fig. 1. An *hhl* electron diffraction pattern from C_{60} buckminsterfullerene [111] plates tilted 35° around the $\mathbf{d}^*_{\bar{1}10}$ reciprocal axis. Note that these patterns, which are obtained from crystals grown by evaporation of a dilute solution of the material in benzene, do not have the twinning characteristics described by Ishiguro & Hirotsu (1992).

phases for 17 unique *hkl* reflections were determined by evaluation of the most probable three- and four-phase invariant sums. Since only one origin-defining reflection is allowed for space group *Fm*3, $\phi_{333} = 0$ was assigned and one additional algebraic quantity $\phi_{113} = a$ was given to evaluate 17 $\sum_2$ triples and 16 quartets above specified *A* and *B* thresholds. The results of this phase determination are outlined in Table 1. Since the final phase set has quantities $a = 0, \pi$, two potential maps must be calculated with a reverse Fourier transform after combining these phase values to observed structure-factor magnitudes. Only one of these maps ($a = \pi$) corresponds to a reasonable structure. The potential map in Fig. 2 was calculated after each reflection *hhl* was permuted through the symmetry-equivalent values, *hlh*, *lhh*, specified by the space group.

The structure in Fig. 2(*a*), which is a projection down the unit cell [001] for one molecular site, is remarkably similar to the initial atomic array described by Fleming *et al.* (1991), resulting from their seeking a structure solution with an averaged C-atom position. In the center of the potential map is a hole, corresponding to the axis of the static

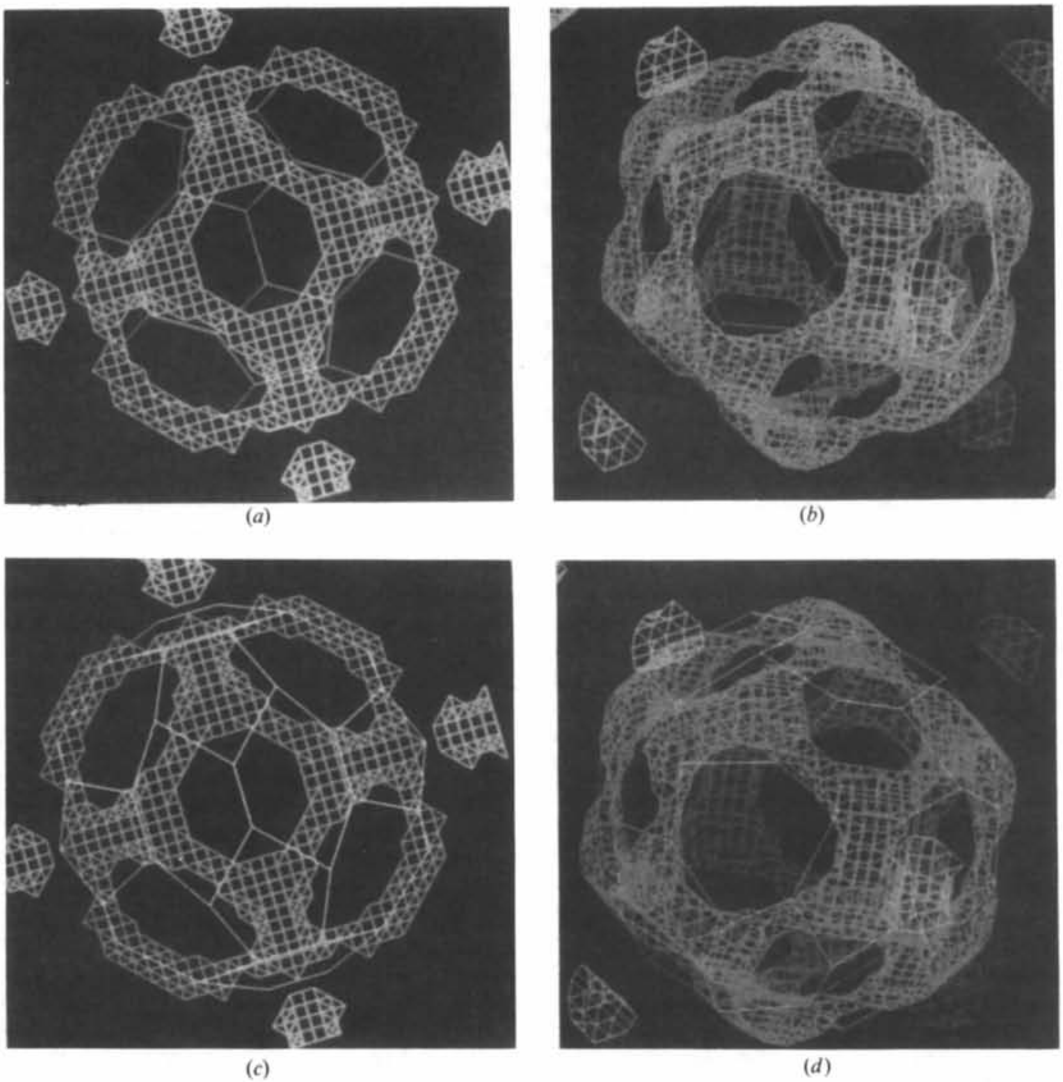

(*a*) (*b*)

(*c*) (*d*)

Fig. 2. Electrostatic potential map calculated for C_{60} buckminsterfullerene (only one molecule of the unit cell) after 17 unique *hhl* reflections are given crystallographic phase values (six of these being symbolic values *a*) by direct evaluation of phase-invariant sums. These crystallographic phases ϕ are combined with observed structure-factor magnitudes $|F_o|$ to permit calculation of the reverse Fourier transform $\rho(r) = V^{-1}\sum|F_o|\cos(\phi)\cos(-2\pi\mathbf{h}\cdot\mathbf{r})$, thus producing the potential map. The phase solution $a = \pi$ is shown. In (*a*) and (*b*), the map density is fit with a regular icosahedron of C atoms. In (*c*) and (*d*), the density is compared to the distorted icosahedral structure found in an earlier X-ray analysis (Fleming *et al.*, 1991).

Table 1. *Crystallographic phases for room-temperature* C_{60} *buckminsterfullerene obtained by direct methods*

0kl	ϕ	*1kl*	ϕ	*2kl*	ϕ	*3kl*	ϕ	*4kl*	ϕ	*5kl*	ϕ
022	*a*†	113	*a*	224	0	333	0‡	444	*a*	553	*a*
		111	0	222	*a*	331	0	400	0	555	0
		115	0			335	*a*	440	*a*§		
		117	*a*					442	0		
		119	0								

† $a = \pi$.
‡ Origin definition.
§ Disagrees with free-rotor model.

Table 2. *Fractional coordinates for* C_{60} *buckminsterfullerene from fitting a regular icosahedron to the observed density in Fig.* 2

	This determination			Model of André *et al.* (1992)*		
	x	*y*	*z*	*x*	*y*	*z*
C1	0.052	0	0.249	0.049	0	0.246
C2	0.105	0.085	0.220	0.101	0.083	0.214
C3	0.185	0.052	0.165	0.184	0.051	0.163

* As shown by these authors, these coordinates can be derived from the two unique C–C bond lengths (taken to be 1.45 and 1.40 Å) and the spherical radius *R* (defined as 3.548 Å).

disorder (coincident with ⟨100⟩), leading to an average *Fm*3*m* cell. The other fourfold distribution of holes in this projection corresponds to the arrangement of six-membered ring centers. Fig. 2(*b*) shows another orientation of this density distribution. From this direct analysis, it appears, therefore, that the electrostatic potential distribution is not continuous over a spherical surface; rather, there seem to be static placements of density to which an oriented molecular model can be fit.

To derive an atomic model to compare to the potential map in Fig. 2, a regular icosahedron of C atoms was generated with a computer-program package for molecular modeling, *SYBYL* (Tripos Associates, Inc., 1991). A fit to the observed density was sought using the sphere radius as the refinable variable. Because the intensity data were imagined to be contaminated by the continuous streaking owing to the stacking disorder (particularly affecting the weaker reflections), the model was first tested against 15 observed structure-factor magnitudes in the region $\sin\theta/\lambda \leq 0.25$ Å^{-1}. When the average C–C bond length is 1.40 Å, the crystallographic residual is $R = 0.34$, but at larger values, *e.g.* 1.47 or 1.54 Å, this residual is reduced to 0.27 or 0.26, respectively, solutions that cannot be distinguished at the 5% significance level when one variable is compared to 15 *hhl* data (Hamilton, 1964). For the structure with an average 1.47 Å C–C bond length and an overall isotropic temperature factor set at $B = 6.0$ Å^2, the agreement of the model in space group *Fm*3 with the total measured *hhl* data set (used for direct phase analysis) is 0.35. If all unique atomic positions are used for the model (Table 2), which is very similar to the one suggested by André *et al.* (1992), $R = 0.30$ in the data limit $\sin\theta/\lambda \leq 0.30$ Å^{-1}. A multislice dynamical scattering calculation based on this static model (Cowley, 1981) improves this agreement to $R = 0.23$ for a crystal thickness $t = 100$ Å.

Problems with the structure analysis

It appears that the fit to the *directly* determined potential map by the distorted icosahedral geometry derived by Fleming *et al.* (1991) is poorer than that found with the regular molecular geometry. As seen in Figs. 2(*c*) and (*d*), the density of this potential map is found to be more regular than the distorted carbon skeleton used in the earlier determination. Again, we emphasize that no molecular model was assumed to determine the density features in Fig. 2, in contrast to the earlier analysis of ambient X-ray data (Fleming *et al.*, 1991) that began with an atomic model.

Does this result really mean that a somewhat ordered structure is observed at room temperature? In order to make a definite decision about this, it is as well to consider possible sources of error in this determination. For example, although the above structure analysis, followed by a correlation for *n*-beam dynamical scattering, may appear to be 'reasonable', there are discrepancies in our observations that have not been mentioned so far. For example, if no corrections are made to the data at all, it is possible to show that structure factors calculated from the distorted molecular geometry reported by Fleming *et al.* (1991), where two atomic positions are assigned average values, actually give a better fit to *all* of the observed *hhl* data ($R = 0.25$) than the kinematical model used above for the dynamical-scattering calculation. There are no limits imposed on the data resolution for this comparison.

How do the measured electron diffraction data compare to those obtained in ambient X-ray diffraction experiments? One major difference between the electron and X-ray data is that the former contain strong even-order I_{h00} values, while in the latter data sets these reflections are nearly extinct (Krätschmer, Lamb, Fostiropoulos & Huffmann, 1990; Heiney *et al.*, 1991). With X-ray data, tests of various packing options produced the best match with a model based on a rotationally disordered sphere of C atoms (André *et al.*, 1992), in direct contradiction to the maps in Fig. 2. As can be seen from the expression for the structure factor for this disordered structure (André *et al.*, 1992),

$$F_{hkl} = F(s) = \sum f_i'(\sin 2\pi r_i s/2\pi r_i s)\exp 2\pi i\mathbf{r}\cdot\mathbf{s},$$

these values are merely the Fourier transform of a uniform disc in any projection. Here, f_i' are the scattering factors corrected for thermal motion and the sinc u term is merely the transform of a rectangle function (but rotated around an axis through its mass center to generate the disc in any projection).

Careful qualitative electron diffraction measurements made recently on thin C_{60} crystals (Van Tendeloo *et al.*, 1992; Amelinckx, Van Heurck, Van Dyck & Van Tendeloo, 1992) have uncovered the cause of the discrepancy in measured axial intensities. The I_{h00} electron diffraction reflections are found to disappear suddenly when the zone axis is slightly offset from the optimal position for excitation, indicating that their anomalous appearance may be caused by incoherent multiple ('secondary') scattering (Cowley, Rees & Spink, 1951), an observation verified in our current work by continuous tilt measurements of electron diffraction patterns at different goniometer settings. The presumed appearance of secondary scattering can also be tested quantitatively. For the three zonal projections where $h00$ reflections are observed, *viz* [110], [310] and [100], it is possible to predict the appearance of these reflections in the diffraction patterns by adding a weighted convolution of intensity mI_h*I_h (Cowley, Rees & Spink, 1951) to the intensity predicted from the rotationally disordered model (André *et al.*, 1992). {Although the [111] stacking faults are a salient disorder in C_{60}, as are the [001] faults in *n*-paraffins, they are not the only ones for either example – see *e.g.* Li *et al.* (1992) or Muto, Van Tendeloo & Amelinckx (1993) for C_{60} or Hu, Dorset & Moss (1989) for *n*-paraffins. It is expected, therefore, that secondary scattering can be found for many crystal orientations.} With the same weight m for all projections, the agreement R with the observed data is 0.19 for [110] (all 36 unique data measured in the experiment) and 0.13 for both [310] (all eight unique data) and [100] (all 11 unique data) when $B = 3.0$ Å^2 is used as the temperature factor in the structure-factor calculation. It is also possible to demonstrate that the values of I_{h00} have somewhat different distributions for each measured zone and that this distribution also is successfully predicted by the secondary-scattering calculation. Combination of these data from all zones to generate a set of 42 unique reflections gives an overall agreement of $R = 0.17$. Since this very simple model gives a better fit to all observed data than the earlier match to a partial data set without recourse to a dynamical-scattering calculation, we believe that the rotationally disordered structure is to be preferred to the static packing of buckminsterfullerene at room temperature – even though a reasonable molecular model can be fit to the observed density. For the phases derived by direct methods, there are no significant differences between the two models. A final listing of observed and calculated structure factors is given in Table 3. It may also be possible, however, that dynamical scattering from the rotationally disordered structure could explain the intense I_{h00} reflections observed. To test this possibility, such a calculation was carried out *via* the phase-grating approximation for a crystal thickness of 100 Å. The model is based on the final phase set in Table 3 for the three sampled projections containing the $h00$ reflections considered in these experiments on elastically bent crystals. While more intense axial reflections can be produced by this calculation, the match to the observed data is not nearly so good as that found with the simpler secondary-scattering correction. Nevertheless, the ultimate origin of these reflections must be identified, *e.g.* in further experiments on a high-voltage electron microscope.

Table 3. *Observed and calculated structure-factor magnitudes for* C_{60} *buckminsterfullerene* (*the latter are corrected for secondary scattering*); (*hkl*) = (*lhk*) = (*klh*) = (*khl*)

hkl	$\lvert F_o\rvert$	$\lvert F_c\rvert$	ϕ	*hkl*	$\lvert F_o\rvert$	$\lvert F_c\rvert$	ϕ
002	1.10	1.02*	π	440	1.31	1.24	0
004	1.02	1.03*	0	442	0.87	0.81	0
006	0.72	0.76*	0	444	1.25	1.14	π
008	0.66	0.52*	π	446	0.45	0.50	0
0,0,10	0.43	0.29*	0	448	0.42	0.31	0
111	2.59	3.54	0	551	1.05	0.98	π
113	2.75	3.38	π	553	0.81	0.60	π
115	1.21	1.82	0	555	0.74	0.58	0
117	0.84	0.98	π	557	0.51	0.76	0
119	0.65	0.51	0	660	0.88	0.56	0
220	4.87	4.58	π	662	0.60	0.60	0
222	2.16	2.77	π	664	0.61	0.45	0
224	1.80	2.09	0	666	0.57	0.30	π
226	1.01	1.11	π	771	0.41	0.28	0
228	0.64	0.57	0	773	0.40	0.26	π
2,2,10	0.34	0.27	π	260	0.84	1.06	π
331	1.57	1.56	0	264	0.64	0.69	π
333	1.99	1.92	0	042	1.82	1.65	0
335	1.00	1.08	π	064	0.88	0.99	π
337	0.54	0.51	0	028	0.51	0.35	0
339	0.41	0.78	0	048	0.86	0.52	0

* Averaged over three zones.

Discussion

It is very curious that a direct analysis of room-temperature electron diffraction intensity data from C_{60} buckminsterfullerene, presuming no molecular model *a priori*, produces an electrostatic potential density distribution that is quite reasonably fit by a regular icosahedron of C atoms packing in a face-centered-cubic lattice. The visual fit of the regular icosahedral model to the density is much better than that of the distorted geometry given earlier (Fleming *et al.*, 1991), with the model bond length very close to the average value given in this X-ray determination. The fractional coordinates are very similar to the ones used in a recent X-ray analysis, assuming a static molecular packing, and the average bond length is quite similar to the average value found in numerous other X-ray and neutron analyses of unsubstituted or substituted C_{60} molecules and also matches the values obtained by gas-phase electron diffraction (Hedberg *et al.*, 1991). Nevertheless, a careful analysis of the intensity data reveals that the molecules must pack in an uncorrelated array, in full agreement with the results from most previous diffraction and spectroscopic determinations. In fact, the initial map, based on a limited phase set, is actually found to be an artefact of series-termination effects. It will be remembered, however, that even the analysis of kinematical room-temperature X-ray data (André *et al.*, 1992) arrived at a number of 'reasonable' structure solutions, as judged by low R-factor values.

The above results underscore the argument that electron diffraction intensity data must be used cautiously when carrying out quantitative structure analyses. There are many possible perturbations to such data sets and one must be absolutely certain which ones are important before settling on a final structural model. The poor fit of the idealized icosahedral structure fit to the density in Fig. 2, in comparison to that given with the grossly distorted geometry, served as a warning that something was very wrong with this analysis. Although some improvement of a lower-resolution subset was provided by an n-beam calculation with the static model, at limited data resolution, the final result was still not very convincing for an analysis of diffraction data from very thin crystals containing only carbon. In retrospect, the presence of secondary scattering is a reasonable perturbation to expect. By analogy to the multilamellar paraffin crystals studied earlier (Cowley, Rees & Spink, 1951) and also to more recent observations of an orthogonal orientation (Hu, Dorset & Moss, 1989), we see that the crystal disorder could easily produce incoherently scattering layers that would cause this phenomenon to occur.

Despite the perturbation, it is very interesting to note that the direct phase determination was not seriously compromised. In fact, both a static and uncorrelated molecular packing lead to nearly the same phase set for this structure in the subset of large $|E_h|$ reflections used to calculate the initial potential map. Although the map in Fig. 2 suggests a 'structure', it is found to become more continuous in density as more phased reflections are used for the Fourier transform to the potential map.

The quantitative electron diffraction structure analysis, therefore, must be taken to support the widely held view of the room-temperature structure of this molecule, which is that there is no strong correlation of angular position in the unit cell.

Research described in this paper was funded by a grant from the National Science Foundation (CHE-91-13899), which is gratefully acknowledged. (This grant is sponsored both by the Theoretical and Computational Chemistry and Polymers Programs of the NSF.)

References

AGAFONOV, V., CÉOLIN, R., SIZARET, P. Y., DWORKIN, A., ANDRÉ, D., SZWARC, H., FABRE, C., RASSAT, A., STRAVER, L., DUGUÉ, J., TAYLOR, R., ZAHAB, A. & BERNIER, P. (1992). *J. Chim. Phys.* **12**, 1879–1886.

AMELINCKX, S., VAN HEURCK, C., VAN DYCK, D. & VAN TENDELOO, G. (1992). *Phys. Status Solidi A*, **131**, 589–604.

ANDRÉ, D., DWORKIN, A., SZWARC, H., CÉOLIN, R., AGAFONOV, V., FABRE, C., RASSAT, A., STRAVER, L., BERNIER, P. & ZAHAB, A. (1992). *Mol. Phys.* **76**, 1311–1317.

BIRKETT, P. R., HITCHCOCK, P. B., KROTO, W., TAYLOR, R. & WALTON, D. R. M. (1992). *Nature (London)*, **357**, 479–481.

CHOW, P. C., JIANG, X., REITER, G., WOCHNER, P., MOSS, S. C., AXE, J. D., HANSON, J. C., MULLAN, R. K., MENG, R. L. & CHU, W. (1992). *Phys. Rev. Lett.* **69**, 2943–2946.

COPLEY, J. R. D., NEUMAN, D. A., CAPPELLETI, R. L., KAMITAKAHARA, W. A., PRINCE, E., COUSTEL, N., MCCAULEY, J. P. JR, MALISZEWSKYJ, N. C., FISCHER, J. E., SMITH, A. B. III, CREEGAN, K. M. & FOX, D. M. (1992). *Physica (Utrecht)*, **B180/181**, 706–708.

COWLEY, J. M. (1981). *Diffraction Physics*, 2nd ed., pp. 238–243. Amsterdam: North-Holland.

COWLEY, J. M., REES, A. L. G. & SPINK, J. A. (1951). *Proc. Phys. Soc. London Sect. A*, **64**, 609–619.

DALY, T. K., BUSEK, P. R., WILLIAMS, P. & LEWIS, C. F. (1993). *Science*, **259**, 1599–1601.

DAVID, W. I. F., IBBERSON, R. M., MATTHEWMAN, J. C., PRASSIDES, K., DENNIS, T. J. S., HARE, J. P., KROTO, H. W., TAYLOR, R. & WALTON, D. R. M. (1991). *Nature (London)*, **353**, 147–149.

DISKO, M. M., BEHAL, S. K., SHERWOOD, R. D., COSANDEY, F., LU, P., CREEGAN, K. M., TINDELL, P. & COX, D. M. (1991). *Proc. 49th Annual Meeting of the Electron Microscopy Society of America, San Francisco*, pp. 1024–1025. San Francisco Press.

DORSET, D. L. (1976). *Acta Cryst.* **A32**, 207–215.

DORSET, D. L. (1991). *Ultramicroscopy*, **38**, 23–40.

DORSET, D. L. (1993). *Microsc. Soc. Am. Bull.* **23**, 99–108.

DORSET, D. L., JAP, B. K., HO, M.-S. & GLAESER, R. M. (1979). *Acta Cryst.* **A35**, 1001–1009.

DOYLE, P. A. & TURNER, P. S. (1968). *Acta Cryst.* **A24**, 390–397.

FAGAN, P. J., CALABRESE, J. C. & MALONE, B. (1991). *Science*, **252**, 1160–1161.

FLEMING, R. M., SIEGRIST, T., MARSH, P. M., HESSEN, B., KORTAN, A. R., MURPHY, D. W., HADDON, R. C., TYCKO, R., DABBAGH, G., MUJSCE, A. M., KAPLAN, M. L. & ZAHURAK, S. M. (1991). *Mater. Res. Soc. Symp. Proc.* **206**, 691–695.

HAMILTON, W. (1964). *Statistics in Physical Science. Estimation, Hypothesis Testing and Least-Squares*, pp. 157–162. New York: Roland.

HAUPTMAN, H. A. (1972). *Crystal Structure Determination. The Role of the Cosine Seminvariants*. New York: Plenum.

HAWKINS, J. M., MAYER, A., LEWIS, T. A., LOREN, S. & HOLLANDER, F. J. (1991). *Science*, **252**, 312–313.

HEDBERG, K., HEDBERG, L., BETHUNE, D. S., BROWN, C. A., DORN, H. C., JOHNSON, R. D. & DEVRIES, M. (1991). *Science*, **254**, 410–412.

HEINEY, P. A., FISCHER, J. F., MCGHIE, A. R., ROMANOW, W. J., DENENSTEIN, A. M., MCCAULEY, J. P. JR, SMITH, A. B. III & COX, D. E. (1991). *Phys. Rev. Lett.* **66**, 2911–2914.

HENRY, N. F. M. & LONSDALE, K. (1969). Editors. *International Tables for X-ray Crystallography*, Vol. I. Birmingham: Kynoch Press.

HU, H. & DORSET, D. L. (1989). *Acta Cryst.* **B45**, 283–290.
HU, H., DORSET, D. L. & MOSS, B. (1989). *Ultramicroscopy*, **27**, 161–170.
ISHIGURO, T. & HIROTSU, Y. (1992). *Jpn. J. Appl. Phys.* **31**, L481–L483.
JAP, B. K. & GLAESER, R. M. (1980). *Acta Cryst.* **A36**, 57.
JOHNSON, R. D., BETHUNE, D. S. & YANNONI, C. S. (1992). *Acc. Chem. Res.* **25**, 169–175.
KRÄTSCHMER, W., LAMB, L. D., FOSTIROPOULOS, K. & HUFFMANN, D. R. (1990). *Nature (London)*, **347**, 354–358.
KROTO, H. W., HEATH, J. R., O'BRIEN, S. C., CURL, R. F. & SMALLEY, R. E. (1985). *Nature (London)*, **318**, 162–163.
LI, J. Q., ZHAO, Z. C., LI, Y. L., ZHU, D. B., GAN, Z. Z. & YIN, D. C. (1992). *Physica (Utrecht)*, **C196**, 135–140.
LIU, S., LU, Y. J., KAPES, M. M. & IBERS, J. A. (1991). *Science*, **254**, 408–410.
MUTO, S., VAN TENDELOO, G. & AMELINCKX, S. (1993). *Philos. Mag.* **B67**, 443–463.
NEUMANN, D. A., COPLEY, J. R. D., CAPPELLETTI, R. L., KANITAKAHARA, W. A., LINDSTROM, R. M., CREEGAN, K. H., COX, D. H., ROMANOW, W. J., COUSTEL, N., MCCAULEY, J. M. JR, MALISZEWSKYJ, N. C., FISCHER, J. E. & SMITH, A. B. III (1991). *Phys. Rev. Lett.* **67**, 3808–3811.
ROGERS, D. (1980). *Theory and Practice of Direct Methods in Crystallography*, edited by M. F. C. LADD & R. A. PALMER, pp. 23–92. New York: Plenum.
SAITO, Y., SUZUKI, N., SHINOHARA, H., HAYASHI, T. & TOMITA. M. (1992). *Ultramicroscopy*, **41**, 1–9.
SCHENK, H. (1991). Editor. *Direct Methods of Solving Crystal Structures NATO ASI Ser. B*, Vol. 274. New York: Plenum.
TEBBE, F. N., HARLOW, R. C., CHASE, D. B., THORN, D. L., CAMPBELL, G. C. JR, CALABRESE, J. C., HERRON, N., YOUNG, R. J. JR & WASSERMAN, E. (1992). *Science*, **256**, 822–825.
TIVOL, W. F., DORSET, D. L., MCCOURT, M. P. & TURNER, J. N. (1993). *Microsc. Soc. Am. Bull.* **23**(1), 91–98.
Tripos Associates, Inc., (1991). *SYBYL Molecular Modeling Software*, Version 5.4. St Louis, MO, USA.
TYCKO, R., DABBAGH, G., FLEMING, R. M., HADDON, R. C., MAKIJA, A. V. & ZAHURAK, S. M. (1991). *Phys. Rev. Lett.* **67**, 1886–1889.
TYCKO, R., HADDON, R. D., DABBAGH, G., GLARUM, S. H., DOUGLASS, D. C. & MUJSCE, A. M. (1991). *J. Phys. Chem.* **95**, 518–520.
VAN TENDELOO, G., OP DE BEECK, M., AMELINCKX, S., BOHR, J. & KRÄTSCHMER, W. (1991). *Europhys. Lett.* **15**, 295–300.
VAN TENDELOO, G., VAN HEURCK, C., VAN LANDUYT, J., AMELINCKX, S., VERHEIJEN, M. A., VAN LOOSDECHT, P. H. M. & MEIJER, G. M. (1992). *J. Phys. Chem.* **96**, 7424–7430.
WANG, S. & BUSEK, P. R. (1991). *Chem. Phys. Lett.* **182**, 1–4.
YANNONI, C. S., JOHNSON, R. D., MEIJER, G., BETHUNE, D. S. & SALEM, J. R. (1991). *J. Phys. Chem.* **95**, 9–10.
YAO, N., KLEIN, C. F., BEHAL, S. K., DISKO, M. M., SHERWOOD, R. D. & COX, D. M. (1992). *Phys. Rev. B.* **45**, 11366–11369.

Acta Cryst. (1994). **A50**, 351–357

Strukturverfeinerung des Kompositkristalls im mehrdimensionalen Raum. II

VON KATSUO KATO

Mukizaishitsu Kenkyusho, 1-1 Namiki, Tsukuba-shi, Ibaraki-ken* 305, *Japan*

(*Eingegangen am* 3. *August* 1993; *angenommen am* 16. *November* 1993)

Abstract

A method for the structure refinement of composite crystals based on the multidimensional formalism of Janner & Janssen [*Acta Cryst.* (1980), **A36**, 408–415] and successfully applied to 'LaCrS$_3$' and $M_{10}Cu_{17}O_{29}$ ($M = Bi_{0.031}Ca_{0.564}Sr_{0.405}$) [Kato (1990). *Acta Cryst.* **B46**, 39–44] is fully described. This method is also applicable to a commensurate composite crystal. Methods for treating atoms in special positions and for calculating bond lengths and angles are presented in detail. In all of these methods, a square matrix P that transforms the subsystem coordinates into the coordinates of the common system plays an important role.

Einleitung

Die von Janner & Janssen (1980*a*,*b*) entwickelte Theorie, einen Kompositkristall als einen periodischen 'Kristall' im mehrdimensionalen Raum zu beschreiben, blieb relativ lange unbeachtet, bis die Synthese einer Reihe von komplexen Sulfiden mit Kompositstruktur (Guemas, Rabu, Meerschaut & Rouxel, 1988; Williams & Hyde, 1988; Wiegers, Meetsma, Haange & de Boer, 1988, 1989; Meetsma, Wiegers, Haange & de Boer, 1989; Oosawa, Gotoh & Onoda, 1989; Wiegers, Meetsma, Van Smaalen, Haange, Wulff, Zeinstra, de Boer, Kuypers, Van Tendeloo, Van Landuyt, Amelinckx, Meerschaut, Rabu & Rouxel, 1989) sowie die Entdeckung von Kompositkristallen unter den supraleitenden komplexen Kupferoxiden und verwandten Verbindungen (Kato, Takayama-Muromachi, Kosuda & Uchida, 1988; McCarron, Subramanian, Calabrese & Harlow, 1988; Siegrist, Schneemeyer, Sunshine, Waszczak & Roth, 1988) den Anlaß boten, diese Theorie als Grundlage einer Strukturverfeinerung anzuwenden. Nach Yamamoto (1993) sind inzwischen zahlreiche Beispiele von Kompositkristallen bekannt geworden und es liegen mehrere Strukturuntersuchungen vor, in denen diese Theorie erfolgreich

---

* Staatliches Institut für Anorganische Materialforschung (National Institute for Research in Inorganic Materials).

Acta Crystallographica Section A
ISSN 0108-7673 © 1994